Mon. Not. R. Astron. Soc. **396,** 2201–2210 (2009) doi:10.1111/j.1365-2966.2009.14870.x

The total and relative contribution of the relevant absorption processes to the opacity of DB white dwarf atmospheres in the UV and VUV regions

Lj. M. Ignjatović,[1,2★] A. A. Mihajlov,[1,2] N. M. Sakan,[1] M. S. Dimitrijević[2,3] and A. Metropoulos[4]

[1]*Institute of Physics, PO Box 57, 11001 Belgrade, Serbia*
[2]*Isaac Newton Institute of Chile, Yugoslavia Branch, Volgina 7, 11160 Belgrade 74, Serbia*
[3]*Astronomical Observatory, Volgina 7, 11160 Belgrade 74, Serbia*
[4]*Theoretical and Physical Chemistry Institute, National Hellenic Research Foundation, Athens, Greece*

Accepted 2009 April 3. Received 2009 February 3; in original form 2008 November 12

ABSTRACT

The main aim of this work is to estimate the total contribution of the processes of He_2^+ molecular ion photodissociation and $He + He^+$ collisional absorption charge exchange to the opacity of DB white dwarf atmospheres, and compare this with the contribution of He^- and other relevant radiative absorption processes included in standard models.

The method for the calculations of the molecular ion He_2^+ photodissociation cross-sections is based on the dipole approximation and quantum-mechanical treatment of the internuclear motion, while the quasi-classical method for describing absorption processes in $He + He^+$ collisions is based on the quasi-static approximation.

Absorption coefficients are calculated in the region $50\,nm \leq \lambda \leq 850\,nm$ and compared with the corresponding coefficients of other relevant absorption processes; the calculations of the optical depth of the atmosphere layers considered are performed in the far-UV and VUV regions; the contribution of the relevant absorption processes to the opacity of DB white dwarf atmospheres is examined.

We examined the spectral ranges in which the total He_2^+ and He^- absorption processes dominate in particular layers of DB white dwarf atmospheres. In addition, we show that in the region of $\lambda \lesssim 70\,nm$ the process of H(1s) atom photoionization is also important, in spite of the fact that the ratio of hydrogen and helium abundances in the DB white dwarf atmosphere considered is $1{:}10^5$.

Key words: atomic processes – molecular processes – radiation mechanisms: general – radiative transfer – stars: atmospheres.

1 INTRODUCTION

The main aim of this work is to obtain a realistic estimation of the total and relative contribution of relevant radiative processes to the opacity, caused by continuous absorption in the far-UV and VUV regions, of particular layers within some DB white dwarf atmospheres, models for which are given in Koester (1980). Namely, such an estimation could be useful for the interpretation of real continual stellar spectra.

Calamida et al. (2008) specified the most important processes contributing to white dwarf absorption coefficients, and the processes involving helium quoted by him, relevant for helium-rich DB white dwarfs, are bound–free absorption of neutral helium and free–free absorption of He^-, considered e.g. by John (1994). Previously, and even now, for the DB white dwarf atmosphere conditions considered here ($T_{\rm eff} = 12\,000$–$14\,000\,K, \log g = 7$–8), the more important of these two processes as a source of continuous absorption is the free–free absorption of He^-, hereinafter named the He^- absorption process. Previously, for the DB white dwarf atmospheres considered ($T_{\rm eff} = 12\,000$–$14\,000\,K, \log g = 7$–8) as the main source of the continuous absorption, the He^- absorption process was treated as follows:

$$\epsilon_\lambda + He + e \Longrightarrow He + e', \quad (1)$$

where ϵ_λ is the energy of a photon with wavelength λ, and e and e′ denote the free electron before and after collision with the He atom. Besides the He^- absorption process, the bound–free absorption processes are usually included, as mentioned by Calamida et al.

★E-mail: ljuba@phy.bg.ac.yu

(2008), including the other relevant reaction channel:

$$\epsilon_\lambda + \begin{cases} \mathrm{He}^*(n, L, S) \\ \mathrm{He}^+ + \mathrm{e} \end{cases} \Longrightarrow \mathrm{He}^+ + \mathrm{e}', \tag{2}$$

where $\mathrm{He}^*(n, L, S)$ is the helium atom in the excited state, n the corresponding principal quantum number, and L and S the quantum numbers of orbital momentum and spin. Continuous absorption opacity due to the processes of He_2^+ molecular ion photodissociation can be written as

$$\epsilon_\lambda + \mathrm{He}_2^+ \Longrightarrow \mathrm{He} + \mathrm{He}^+, \tag{3}$$

and $\mathrm{He} + \mathrm{He}^+$ collisional absorption charge exchange as

$$\epsilon_\lambda + \mathrm{He} + \mathrm{He}^+ \Longrightarrow \begin{cases} \mathrm{He}^+ + \mathrm{He} \\ \mathrm{He} + \mathrm{He}^+ \end{cases}, \tag{4}$$

where $\mathrm{He} \equiv \mathrm{He}(1s^2)$, $\mathrm{He}^+ \equiv \mathrm{He}^+(1s)$ and $\mathrm{He}_2^+ \equiv \mathrm{He}_2^+(X^2\Sigma_u^+)$ were neglected in DB white dwarf atmosphere modelling up to the beginning of the 1990s. However, Mihajlov & Dimitrijević (1992) and Mihajlov, Dimitrijević & Ignjatović (1994a), using the DB white dwarf atmosphere models of Koester (1980), demonstrated that at least for $T_{\mathrm{eff}} < 16\,000$ K these processes should contribute to the opacity in the optical region. In these papers the absorption coefficients for both processes (3) and (4) have been determined within the semiclassical (quasi-static) method developed by Bates (1952).

Processes (3) and (4) were considered later in Stancil (1994) but, in contrast to Mihajlov & Dimitrijević (1992) and Mihajlov et al. (1994a), the photodissociation channel (3) was treated completely quantum-mechanically. A significant result of this paper was the inclusion of the absorption coefficients for processes (3) and (4) obtained by Stancil (1994) in modern DB white dwarf atmosphere modelling codes (Bergeron, Wesemael & Beauchamp 1995; Beauchamp et al. 1996; Beauchamp, Wesemael & Bergeron 1997). This inclusion was probably accelerated by the fact that Stancil (1994) suggest the absolute domination of processes (3) and (4), at least in the region shown ($\lambda \leq 500$ nm), in comparison with the He^- absorption processes (1). In connection with this, one should emphasize that such a suggestion is based only on fig. 7 of Stancil (1994), in relation to the model with $\log g = 8, T_{\mathrm{eff}} = 12\,000$ K from Koester (1980). Moreover, this figure shows the behaviour with λ of the He^- and He_2^+ total absorption coefficients determined for only one value of the Rosseland optical depth ($\tau = 1$). However, one can see in this figure that the He^+ density is 10 times larger than the electron density, so that the curve of the He_2^+ total absorption coefficient is obtained with He^+ ion densities (needed for the calculation) ten times larger than in local thermodynamic equilibrium (LTE), which is assumed in the basic model used (Koester 1980). According to this, the real curve should lie much lower and cross the curve of the He^- absorption coefficient. Consequently, the question of the relative importance of particular absorption processes in DB white dwarf atmospheres remains open. This justifies the fact that in some modern investigations of DB white dwarf atmospheres these processes are neglected.

The results from Mihajlov et al. (1994a), obtained for one Koester model ($\log g = 8$ and $T_{\mathrm{eff}} = 12\,000$ K), have already provided a more realistic picture of the relative importance of He^- and He_2^+ total absorption processes, at least in the region $\lambda \geq 300$ nm. From these results follows the above-mentioned crossing of the curves for He^- and He_2^+ absorption coefficients. In a following paper (Mihajlov et al. 1995), the relative importance of He_2^+ and other relevant absorption processes in the region $\lambda \geq 200$ nm was examined for several of Koester's (1980) models ($T_{\mathrm{eff}} = 12\,000, 14\,000, 16\,000$ K, $\log g = 7, 8$). It was shown that, in all cases considered, the contribution to opacity of the processes of He_2^+ molecular ion photodissociation and $\mathrm{He} + \mathrm{He}^+$ collisional absorption charge exchange combined is close to or at least comparable with the contribution of the He^- absorption processes (1) and atomic absorption processes (2).

The continuation of our investigations of processes (3) and (4) was inspired by the results obtained in connection with the processes of H_2^+ molecular ion photodissociation and $\mathrm{H} + \mathrm{H}^+$ collisional absorption charge exchange in the solar atmosphere. Here, we recall that in Mihajlov & Dimitrijević (1986), Mihajlov, Dimitrijević & Ignjatović (1993) and Mihajlov et al. (1994b) the relative importance of the absorption processes was investigated:

$$\epsilon_\lambda + \mathrm{H}_2^+ \Longrightarrow \mathrm{H} + \mathrm{H}^+, \tag{5a}$$

$$\epsilon_\lambda + \mathrm{H} + \mathrm{H}^+ \Longrightarrow \begin{cases} \mathrm{H}^+ + \mathrm{H} \\ \mathrm{H} + \mathrm{H}^+ \end{cases}, \tag{5b}$$

where $\mathrm{H} \equiv \mathrm{H}(1s)$ and $\mathrm{H}_2^+ \equiv \mathrm{H}_2^+(X^2\Sigma_g^+)$, in the optical region of λ in the solar photosphere and lower chromosphere. The efficiency of these processes was compared with the efficiency of the known absorption processes that have already been treated in the literature (Mihalas 1978), namely

$$\epsilon_\lambda + \mathrm{H}^- \Longrightarrow \mathrm{H} + \mathrm{e}', \tag{6a}$$

$$\epsilon_\lambda + \mathrm{H} + \mathrm{e} \Longrightarrow \mathrm{H} + \mathrm{e}', \tag{6b}$$

$$\epsilon_\lambda + \begin{cases} \mathrm{H}^*(n) \\ \mathrm{H}^+ + \mathrm{e} \end{cases} \Longrightarrow \mathrm{H}^+ + \mathrm{e}', \tag{6c}$$

where H^- is the negative hydrogen ion in the ground state, and $\mathrm{H}^*(n)$ is the hydrogen atom in the excited state, with the principal quantum number $n \geq 2$. It was shown that the relative contribution of processes (5) to the opacity of the layers of the solar atmosphere considered in the visible and near-UV regions of continual spectra does not exceed 10–12 per cent. Such a relatively small contribution is a consequence of the presence of the highly efficient absorption process (6a) in the solar atmosphere. However, in Mihajlov et al. (2007) it was shown that the relative contribution of processes (5) to the opacity of particular layers of the solar atmosphere in the far-UV and VUV regions reaches almost 90 per cent of the total contribution of all concurrent processes (6a), (6b) and (6c). This result means that processes (5) in the short-wave region become equally as important as process (6a).

It should be noted in this context that in Mihajlov & Dimitrijević (1992) and Mihajlov et al. (1994a, 1995) it was shown that the relative contribution of processes (4) in some DB white dwarfs ($T_{\mathrm{eff}} = 12\,000$ K, $\log g = 8$) is around 50 per cent, i.e. several times larger than the related contribution of processes (5a) and (5b) in the solar atmosphere. This difference in comparison with the solar atmosphere is due to the absence in DB white dwarf atmospheres of a highly efficient absorption process similar to process (6a) in the solar atmosphere. The above-mentioned work suggests that the relative contribution of absorption processes (3) and (4) to the opacity of DB white dwarf atmospheres in the far-UV and VUV regions ($\lambda < 200$ nm) of continual spectra could be considerably larger than the relative contribution of absorption processes (5) to the opacity of the solar atmosphere.

For this reason, we continued our previous investigations (Mihajlov & Dimitrijević 1992; Mihajlov et al. 1994a, 1995) of

processes (3) and (4) in DB white dwarf atmospheres in the far-UV and VUV regions. In accordance with the aims of this paper, the temperature and particle densities in particular layers should be known. In spite of the fact that Koester's DB white dwarf atmospheric models were published in 1980, only recently were the data needed for such estimation presented, so that they are used for example by Marsh, Nelemans & Steeghs (2004).

In order to examine qualitatively the influence of absorption processes (3) and (4) on the opacity of DB white dwarf atmospheres, Koester's (1980) models with $T_{\rm eff} = 12\,000$ K and $\log g = 8$ and 7 and with $T_{\rm eff} = 14\,000$ K and $\log g = 8$ were used in this work. Here the necessary calculations of absorption coefficients characterizing processes (4) were performed. The determination of these coefficients was obtained from the potential curves of molecular ion He_2^+ in the $X^2\Sigma_u^+$ and $A^2\Sigma_g^+$ states, as well as the corresponding dipole matrix elements, which were precisely calculated during this research. These characteristics of He_2^+ are presented here.

In order to determine the relative efficiency of processes (4) in the UV and VUV regions for particular DB white dwarf atmosphere layers, the corresponding absorption coefficients will be compared with the absorption coefficients that characterize the concurrent processes (1) and (2) for 51 nm $\leq \lambda \leq$ 400 nm. The lower boundary of this region was taken as $\lambda = 51$ nm, which is close to the He atom ionization boundary $\lambda_{\rm He} \cong 50.14$ nm, below which the photoionization of the He atom absolutely dominates in comparison with all other absorption processes.

Also, we will consider here the hydrogen photoionization process

$$\epsilon_\lambda + {\rm H} \Longrightarrow {\rm H}^+ + {\rm e}'. \tag{7}$$

Although according to Koester (1980) the ratio of hydrogen and helium abundances in the considered DB white dwarf atmospheres is $1{:}10^5$, our estimations showed that process (7) could play a certain role for $\lambda < \lambda_{\rm H}$, where $\lambda_{\rm H} \cong 91.13$ nm is the H atom ionization boundary.

As a quantitative characteristic of the contribution of processes (4) to the opacity of a DB white dwarf atmosphere, the increase of the optical depth of particular atmosphere layers caused by these processes was taken here. The corresponding calculations were performed for each of the cases mentioned, in the same region of λ. Also, this increase was compared with the optical depth of the layers considered caused by absorption processes (4), (1), (2) and (7) together.

Here we used the models of DB white dwarf atmospheres from Koester (1980) already mentioned, since they provide all the required data on particle densities and temperatures, in particular DB white dwarf atmospheric layers. In all further discussion it was taken into account that these models assumed the existence of local thermodynamical equilibrium (LTE).

2 CHARACTERISTICS OF PHOTODISSOCIATION AND ION–ATOM ABSORPTION PROCESSES

2.1 The photodissociation cross-section

The photodissociation process (3) is characterized here by the corresponding average cross-section $\sigma_{\rm phd}(\lambda, T)$. This cross-section is defined by

$$\sigma_{\rm phd}(\lambda, T) = \frac{\sum_J \sum_v g_{v,J}\,(2J+1){\rm e}^{-E_{v,J}/(kT)}\,\sigma_{v,J}(\lambda)}{\sum_J \sum_v g_{v,J}\,(2J+1){\rm e}^{-E_{v,J}/(kT)}}, \tag{8}$$

where v and J are the vibrational and rotational quantum numbers of the individual rovibrational states (v, J) of the molecular ion $He_2^+(X^2\Sigma_u^+)$, $\sigma_{v,J}(\lambda)$ the partial photodissociation cross-sections of these states, $E_{v,j}$ and $g_{v,j}(2J+1)$ the corresponding energies with respect to the ground rovibrational state and statistical weights, while factor $g_{v,j}$ describes the influence of nuclear spin. Here we consider that this influence is negligible at temperatures much higher than room temperature (see e.g. Patch 1969; Lebedev & Presnyakov 2002). Since for DB white dwarf atmospheres temperatures $T \gtrsim 8000$ K are relevant, for further consideration we assume that $g_{v,j} = 1$.

Within the dipole approximation the partial cross-sections $\sigma_{v,j}(\lambda)$ are given by the expressions

$$\sigma_{v,J}(\lambda) = \frac{8\pi^3}{3\lambda}\left[\frac{J+1}{2J+1}|D_{E,J+1;v,J}|^2 + \frac{J}{2J+1}|D_{E,J-1;v,J}|^2\right], \tag{9}$$

where $D_{E,J+1;v,J}$ and $D_{E,J-1;v,J}$ are the radial matrix elements given by the relations

$$D_{E,J;v,J'} = < \Psi_{2;E,J'}(R)|D_{12}(R)|\Psi_{1;v,J}(R) >, \quad J = J' \pm 1, \tag{10}$$

$$D_{12}(R) = |\boldsymbol{D}_{12}(R)|, \qquad \boldsymbol{D}_{12}(R) = < 1|\boldsymbol{D}(R)|2 >, \tag{11}$$

where R is the internuclear distance, $\boldsymbol{D}(R)$ the operator of electron dipole momentum, and $|1\rangle \equiv X^2\Sigma_u^+$ and $|2\rangle \equiv A^2\Sigma_g^+$ are the ground and first excited electronic states of the molecular ion He_2^+ with the potential curves $U_1(R)$ and $U_2(R)$, respectively. $\Psi_{1;v,j}(R)$ and $\Psi_{2;E,J'}(R)$ denote the adiabatic nuclear radial wavefunctions of the bound state (v, J) in the potential $U_1(R)$ and the continual state (E, J') in the potential $U_2(R)$ respectively, with

$$E = E_{v,J} + \epsilon_\lambda. \tag{12}$$

It is assumed that the wavefunctions $\Psi_{1;v,j}(R)$ and $\Psi_{2;E,J'}(R)$ satisfy the standard orthonormalization conditions.

In the hydrogen case the whole problem was much simpler, because all the required characteristics of molecular ion H_2^+ were already well known for $0 \leq R \leq \infty$. However, in the helium case the situation was quite different: the calculation of $\sigma_{\rm phd}(\lambda, T)$ required the usage of incompatible data from different sources and, consequently, the introduction of additional approximations (e.g. the characteristics of the He_2^+ molecular ion are determined in Stancil, Bab & Dalgarno (1993) on the basis of data from six different articles). This situation has not changed until now.

That is why within this research a special effort was made to determine the potential energies $U_1(R)$ and $U_2(R)$ and the matrix element $D_{12}(R)$ consistently over a wide region of R. The calculations of these quantities were performed under D_{2h} symmetry using the MOLPRO package of programs (Werner et al. 2006). They were performed at the multi-reference configuration interaction (MRCI) level using multi-configuration self-consistent field (MCSCF) orbitals with the cc-pv5z basis set of Dunning (1989) and Kendall, Dunning & Harrison (1992). We started at the self-consistent field (SCF) level with the ground-state electron configuration $a_g^2 b_{1u}^1$. The active space at the MCSCF step contained $3a_g$ and $3b_{1u}$ orbitals without any closed or core orbitals (all three electrons were involved). The potential curves $U_1(R)$ and $U_2(R)$ obtained are presented in Fig. 1, and the dipole matrix element $D_{12}(R)$ in Fig. 2. Unfortunately, it is not possible to compare the potential curves presented in this paper with the potential curves used in Stancil et al. (1993) and Stancil (1994), since they are not given there. We note that in Stancil et al. (1993) and Stancil (1994) the data from earlier

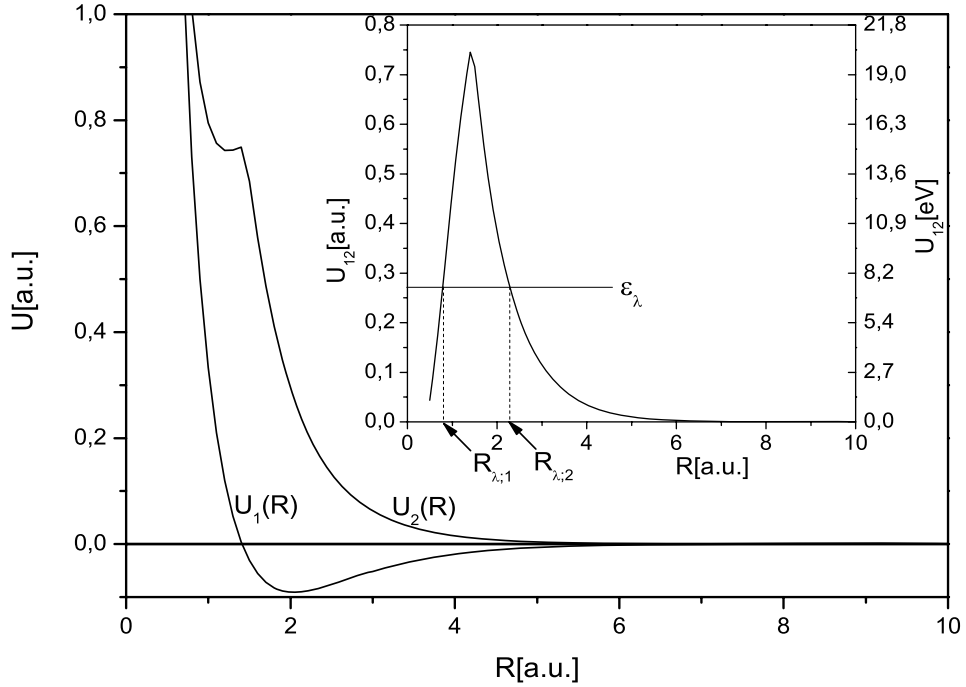

Figure 1. The potential curves of the molecular ion He_2^+: $U_1(R)$ corresponds to the ground electronic state $X^2\Sigma_u^+$, and $U_2(R)$ to the first excited electronic state $A^2\Sigma_g^+$; $U_{12}(R) = U_2(R) - U_1(R)$, 1 au $\approx$ 27.21 eV.

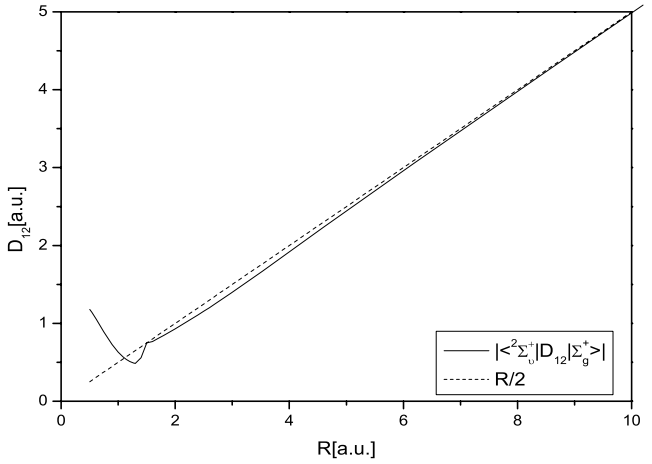

Figure 2. The matrix element $D_{12}(R)$ for the transition between the electronic states $X^2\Sigma_u^+$ and $A^2\Sigma_g^+$ of the ion He_2^+.

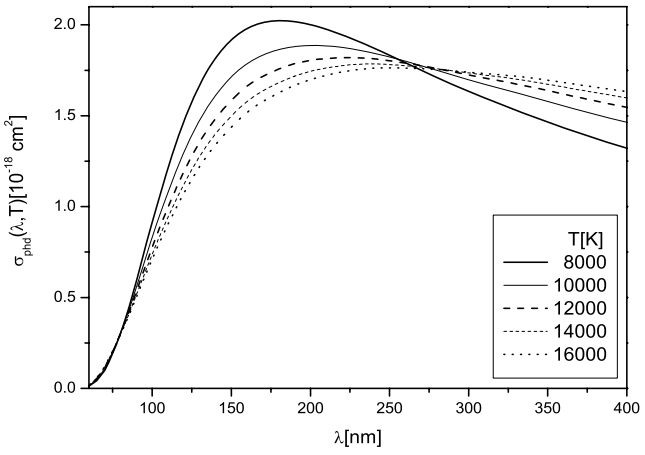

Figure 3. The behaviour of the average cross-section $\sigma_{phd}(\lambda, T)$ for photodissociation of the He_2^+ molecular ion, as a function of λ, for 8000 K $\leq T \leq$ 16 000 K.

papers of Metropoulos and coworkers (Metropoulos, Nicolaides & Buenker 1987; Metropoulos & Nicolaides 1991; Metropoulos et al. 1992) had an especially important role.

With the results obtained here, the required potential curves are self-consistent, since we now have the quantities $U_1(R)$, $U_2(R)$ and $D_{12}(R)$ within a wide region of R, which is enough for determination of the cross-section $\sigma_{phd}(\lambda, T)$ and the corresponding coefficient $K_{ia}^{(a)}(\lambda, T)$ for the photodissociation processes (3). The results obtained are illustrated in Fig. 3, where the behaviour of $\sigma_{phd}(\lambda, T)$ in the UV and VUV regions for T = 8000, 10 000, 12 000, 14 000 and 16 000 K is shown.

From Fig. 3 one can see that the behaviour of $\sigma_{phd}(\lambda, T)$ is similar to the behaviour of photodissociation cross-sections in the hydrogen case obtained in Mihajlov et al. (2007). Because of that in, the helium case one should also expect the increase of absorption caused by ion–atom processes (4) in the short-wave region (λ < 300 nm).

2.2 The partial absorption coefficients

The efficiencies of the photodissociation process (3) and the charge-exchange absorption process (4) are characterized separately by the partial spectral absorption coefficients $\kappa_{ia}^{(a)}(\lambda) \equiv \kappa_{ia}^{(a)}[\lambda; T, N(He_2^+)] = \sigma_{phd}(\lambda, T)N(He_2^+)$ and $\kappa_{ia}^{(b)}(\lambda) \equiv \kappa_{ia}^{(b)}[\lambda; T, N(He), N(He^+)]$ where T, $N(He_2^+)$, $N(He)$ and $N(He^+)$ are the local temperature and the densities of $He_2^+(X^2\Sigma_u^+)$, He and He^+ in the layer of the DB white dwarf atmosphere considered. Following our previous paper (Mihajlov et al. 2007) and assuming the existence of LTE, we will take the photodissociation coefficient $\kappa_{ia}^{(a)}(\lambda)$ in an equivalent form suitable for further consideration,

namely

$$\kappa_{\rm ia}^{\rm (a)}(\lambda) = K_{\rm ia}^{\rm (a)}(\lambda, T) N({\rm He}) {\rm N}({\rm He}^+), \tag{13}$$

$$K_{\rm ia}^{\rm (a)}(\lambda, T) = \sigma_{\rm phd}(\lambda, T)\, \chi_{\rm ia}(T), \tag{14a}$$

$$\chi_{\rm ia}(T) = \frac{N({\rm He}_2^+)}{N({\rm He}) {\rm N}({\rm He}^+)}. \tag{14b}$$

Here the photodissociation cross-section $\sigma_{\rm phd}(\lambda, T)$ is given by equations (8)–(12), and the quantity $\chi_{\rm ia}$, which contains the density $N({\rm He}_2^+)$, is determined from the law of mass action,

$$\chi^{-1}(T) = \left(\frac{\mu k T}{2\pi\hbar^2}\right)^{\frac{3}{2}} \frac{g({\rm He}) g({\rm H}^+)}{\sum\limits_J \sum\limits_v g_{v,J}(2J+1){\rm e}^{-E_{v,J}/(kT)}} \exp\left(-\frac{D}{kT}\right), \tag{15}$$

where μ and D are the reduced mass and the dissociation energy of the molecular ion He_2^+, and $g({\rm He}) = 1$ and $g({\rm He}^+) = 2$ are the statistical weights of the atom He and ion He^+.

The charge-exchange absorption coefficient $\kappa_{\rm ia}^{\rm (b)}(\lambda)$ is defined by

$$\kappa_{\rm ia}^{\rm (b)}(\lambda) = K_{\rm ia}^{\rm (b)}(\lambda, T) N({\rm He}) N({\rm He}^+), \tag{16}$$

where the coefficient $K_{\rm ia}^{\rm (b)}(\lambda, T)$ is determined here by the semiclassical method developed in Bates (1952) on the basis of the quasi-static approximation (see Mihajlov et al. 1994a; Mihajlov et al. 1995, 2007). Within this method, only the λ region where the equation

$$U_{12}(R) \equiv U_2(R) - U_1(R) = \epsilon_\lambda \tag{17}$$

has real roots is considered. Consequently, in the helium case the quasi-static method is applicable in the region $\lambda \gtrsim 62$ nm where this equation has two real roots (see Fig. 1), $R_{\lambda;1}$ and $R_{\lambda;2} > R_{\lambda;1}$. In Mihajlov et al. (1995), where the optical region of λ was treated, only the larger of these roots has been taken into account. However, in the far-UV and VUV regions both roots should be taken into account. Consequently, we will take here $K_{\rm ia}^{\rm (b)}(\lambda, T)$ in the form

$$K_{\rm ia}^{\rm (b)}(\lambda, T) = 0.62 \times 10^{-42} \sum_{i=1}^{2} \frac{\left[\dfrac{2D_{12}(R_{\lambda;i})}{e R_{\lambda;i}}\right]^2}{\gamma(R_{\lambda;i})} \times \left(\frac{R_{\lambda;i}}{a_0}\right)^4 \exp\left[-\frac{U_1(R_{\lambda;i})}{kT}\right] \xi(R_{\lambda;i}), \tag{18}$$

$$\gamma(R_{\lambda;i}) = \left| \frac{{\rm d} \ln\left[\dfrac{U_{12}(R)}{2Ry}\right]}{{\rm d}(R/a_0)} \right|_{R=R_{\lambda;i}}, \tag{19a}$$

$$\xi(R_{\lambda;i}) = \begin{cases} 1, & U_1(R_{\lambda;i}) \geq 0, \\ \dfrac{\Gamma\left(\dfrac{3}{2}; -\dfrac{U_1(R_{\lambda;i})}{kT}\right)}{\Gamma\left(\dfrac{3}{2}\right)}, & U_1(R_{\lambda;i}) < 0, \end{cases} \tag{19b}$$

where e and a_0 are the electron charge and the atomic unit of length, and $K_{\rm ia}^{\rm (b)}(\lambda, T)$ is expressed in $\rm cm^5$.

2.3 The total absorption coefficient

The efficiency of absorption processes (3) and (4) together is characterized by the total spectral absorption coefficient $\kappa_{\rm ia}(\lambda) \equiv \kappa_{\rm ia}[\lambda; T, N({\rm He}), N({\rm He}^+)]$ given by: $\kappa_{\rm ia}(\lambda) = \kappa_{\rm ia}^{\rm (a)}(\lambda) + \kappa_{\rm ia}^{\rm (b)}(\lambda)$. Using equations (13) and (16) for $\kappa_{\rm ia}^{\rm (a)}(\lambda)$ and $\kappa_{\rm ia}^{\rm (b)}(\lambda)$, we will take $\kappa_{\rm ia}(\lambda)$ in the form

$$\kappa_{\rm ia}(\lambda) = K_{\rm ia}(\lambda, T) N({\rm He}) N({\rm He}^+), \tag{20a}$$

$$K_{\rm ia}(\lambda, T) = K_{\rm ia}^{\rm (a)}(\lambda, T) + K_{\rm ia}^{\rm (b)}(\lambda, T), \tag{20b}$$

where $K_{\rm ia}^{\rm (a)}(\lambda, T)$ is given by equations (14) and (8), and $K_{\rm ia}^{\rm (b)}(\lambda, T)$ by equations (18) and (19). For the comparison of the efficiency of processes (4) with the efficiencies of the concurrent processes (1), (2) and (7) only the total absorption coefficients $\kappa_{\rm ia}(\lambda)$ and $K_{\rm ia}(\lambda, T)$ are needed. Table 1 illustrates the behaviour of the coefficient $K_{\rm ia}(\lambda, T)$ for $8000\,{\rm K} \leq T \leq 20\,000\,{\rm K}$ and $50\,{\rm nm} \leq \lambda \leq 850\,{\rm nm}$. Since the values of $K_{\rm ia}(\lambda, T)$ are determined by the new characteristics of the molecular ion $He_2^+(X^2\Sigma_u^+)$, this table covers not only the far-UV and VUV region but also the optical region.

The relative contribution of processes (3) and (4) can be characterized by the branch coefficients

$$X^{\rm (a)}(\lambda, T) = \frac{\kappa_{\rm ia}^{\rm (a)}(\lambda, T)}{\kappa_{\rm ia}(\lambda, T)} = \frac{K_{\rm ia}^{\rm (a)}(\lambda, T)}{K_{\rm ia}(\lambda, T)}, \tag{21a}$$

$$X^{\rm (b)}(\lambda, T) = \frac{\kappa_{\rm ia}^{\rm (b)}(\lambda, T)}{\kappa_{\rm ia}(\lambda, T)} \equiv 1 - X^{\rm (a)}(\lambda, T). \tag{21b}$$

The behaviour of $X^{\rm (a)}(\lambda, T)$ is illustrated by Table 2. This table shows that within the region of λ considered both processes (3) and (4) have to be taken into account together, since neither of them dominates.

The efficiency of processes (4) within a DB white dwarf atmosphere is compared here with the efficiency of the concurrent absorption processes (1) and (2), which are characterized by the spectral absorption coefficients $\kappa_{\rm ea}(\lambda)$ and $\kappa_{\rm ei}(\lambda)$, namely

$$\begin{aligned} \kappa_{\rm ea}(\lambda) &= K_{\rm ea}(\lambda, T) N_{\rm e} N({\rm He}), \\ \kappa_{\rm ei}(\lambda) &= K_{\rm a;ei}(\lambda, T) N_{\rm e} N({\rm He}^+), \end{aligned} \tag{22}$$

$$\begin{aligned} K_{\rm a;ei}(\lambda, T) &= \sum_{n \geq 2, L, S} \sigma_{nLS}(\lambda) \chi_{nLS}(T) + K_{\rm ei}(\lambda, T), \\ \chi_{nLS}(T) &= \frac{N[{\rm He}^*(n, L, S)]}{N_{\rm e} N({\rm He}^+)}. \end{aligned} \tag{23}$$

where $K_{\rm ea}(\lambda, T)$ and $K_{\rm ei}(\lambda, T)$ are the rate coefficients that describe absorption by (e + He) and (e + He^+) collision systems. $N_{\rm e}$ and $N[{\rm He}^*(n, L, S)]$ denote the densities of the free electrons and the excited atoms $He^*(n, L, S)$, and $\sigma_{nLS}(\lambda)$ the corresponding excited atom photoionization cross-section. It was found that in all cases considered the absorption processes (2) play a minor role in comparison with the electron–atom process (1). This is a consequence of the fact that helium plasma in the layers of the DB white dwarf atmosphere considered is weakly ionized. The relative efficiency of processes (4) with respect to processes (1) and (2) together is characterized by the parameter $F_{\rm He}(\lambda)$, defined by

$$\begin{aligned} F_{\rm He}(\lambda) &= \frac{\kappa_{\rm ia}(\lambda)}{\kappa_{\rm ea}(\lambda) + \kappa_{\rm ei}(\lambda)} \\ &= \frac{K_{\rm ia}(\lambda, T)\left[N({\rm He}^+)/N_{\rm e}\right]}{K_{\rm ea}(\lambda, T) + K_{\rm ei}(\lambda, T)\left[N({\rm He}^+)/N({\rm He})\right]}. \end{aligned} \tag{24}$$

In calculations of $F_{\rm He}(\lambda)$, the coefficient $K_{\rm ea}(\lambda, T)$ was determined by means of the data from Somerville (1965), and $K_{\rm a;ei}(\lambda, T)$ by means of expressions from Sobel'man (1979) for the partial

Table 1. The total absorption coefficient $K_{\rm ia}(\lambda, T)$.

λ (nm)	$K_{\rm ia}$(cm^5)						
	8000 K	10 000 K	12 000 K	14 000 K	16 000 K	18 000 K	20 000 K
50	.241E−44	.145E−44	.987E−45	.727E−45	.564E−45	.454E−45	.375E−45
55	.418E−43	.258E−43	.179E−43	.133E−43	.104E−43	.842E−44	.700E−44
60	.195E−41	.118E−41	.811E−42	.600E−42	.467E−42	.377E−42	.312E−42
65	.126E−40	.946E−41	.793E−41	.704E−41	.646E−41	.607E−41	.578E−41
70	.214E−40	.141E−40	.108E−40	.895E−41	.779E−41	.701E−41	.646E−41
80	.576E−40	.332E−40	.230E−40	.177E−40	.146E−40	.125E−40	.111E−40
90	.106E−39	.564E−40	.369E−40	.273E−40	.218E−40	.183E−40	.159E−40
100	.161E−39	.815E−40	.518E−40	.375E−40	.294E−40	.243E−40	.209E−40
125	.275E−39	.135E−39	.838E−40	.597E−40	.462E−40	.379E−40	.323E−40
150	.336E−39	.167E−39	.105E−39	.752E−40	.586E−40	.482E−40	.413E−40
175	.357E−39	.183E−39	.117E−39	.854E−40	.672E−40	.559E−40	.482E−40
200	.360E−39	.191E−39	.126E−39	.931E−40	.743E−40	.624E−40	.542E−40
250	.343E−39	.196E−39	.135E−39	.103E−39	.846E−40	.724E−40	.639E−40
300	.322E−39	.195E−39	.140E−39	.110E−39	.922E−40	.802E−40	.718E−40
350	.302E−39	.192E−39	.143E−39	.115E−39	.980E−40	.865E−40	.783E−40
400	.288E−39	.192E−39	.146E−39	.120E−39	.104E−39	.928E−40	.847E−40
450	.276E−39	.190E−39	.148E−39	.124E−39	.108E−39	.977E−40	.900E−40
500	.267E−39	.189E−39	.151E−39	.128E−39	.113E−39	.103E−39	.953E−40
550	.261E−39	.190E−39	.154E−39	.132E−39	.118E−39	.108E−39	.100E−39
600	.260E−39	.193E−39	.158E−39	.137E−39	.124E−39	.114E−39	.106E−39
650	.258E−39	.195E−39	.162E−39	.142E−39	.128E−39	.118E−39	.111E−39
700	.256E−39	.197E−39	.165E−39	.146E−39	.132E−39	.123E−39	.116E−39
750	.255E−39	.199E−39	.168E−39	.150E−39	.137E−39	.128E−39	.121E−39
800	.251E−39	.199E−39	.170E−39	.152E−39	.140E−39	.131E−39	.124E−39
850	.251E−39	.201E−39	.173E−39	.156E−39	.144E−39	.135E−39	.129E−39

Table 2. The branch coefficient $X^{(a)}(\lambda, T)$.

λ (nm)	$X^{(a)}$						
	8000 K	10 000 K	12 000 K	14 000 K	16 000 K	18 000 K	20 000 K
65	0.560	0.444	0.360	0.298	0.251	0.214	0.186
80	0.861	0.778	0.699	0.628	0.566	0.511	0.464
100	0.922	0.859	0.793	0.728	0.669	0.615	0.566
150	0.927	0.866	0.801	0.738	0.679	0.625	0.576
200	0.904	0.833	0.761	0.694	0.633	0.578	0.530
300	0.825	0.735	0.654	0.583	0.522	0.470	0.425
400	0.745	0.645	0.561	0.492	0.434	0.387	0.347
500	0.673	0.570	0.487	0.421	0.368	0.325	0.289
600	0.602	0.502	0.424	0.363	0.316	0.277	0.246
700	0.546	0.449	0.376	0.320	0.276	0.241	0.213
800	0.501	0.407	0.337	0.285	0.245	0.213	0.187

photoionization cross-section $\sigma_{nLS}(\lambda)$ and the free–free electron–ion absorption coefficient $K_{\rm ei}(\lambda, T)$. The coefficient $K_{\rm ia}(\lambda, T)$ is determined by equations (20), (14) and (18), but all necessary values of $K_{\rm ia}(\lambda, T)$ can be obtained by means of Table 1.

As in Mihajlov et al. (1994a, 1995), the parameter $F_{\rm He}(\lambda)$ is treated as a function of $\log\tau$, where τ is Rosseland optical depth of the atmosphere layer considered (Mihalas 1978). The values of $\log\tau$ are taken from Koester (1980). The behaviour of $F_{\rm He}(\lambda; \log\tau)$ is illustrated in Figs 4, 5 and 6, for atmospheres of DB white dwarfs with $T_{\rm eff} = 12\,000$ K and $\log\tau = 8$, $T_{\rm eff} = 12\,000$ K and $\log\tau = 7$, and $T_{\rm eff} = 14\,000$ K and $\log\tau = 8$, respectively. According to the expectations, the relative efficiency of absorption processes (4) in the far-UV and VUV regions was increased several times with respect to the optical region. The result is that processes (4) in the region $80\,{\rm nm} \lesssim \lambda \lesssim 200\,{\rm nm}$ dominate in comparison with the concurrent processes (1) and (2) in significant parts of DB white dwarf atmospheres (maximal values of $F_{\rm He} \approx 2.5$). From Figs 4 and 6 one can see that the relative efficiency of processes (4) weakly decreases (∼5 per cent) with the decrease of $\log g$ from 8 to 7 for $T_{\rm eff} = 12\,000$ K, while the shape of curves $F_{\rm He}(\lambda; \log\tau)$ stays practically the same. However, Fig. 5 shows that increasing $T_{\rm eff}$ from 12 000 K to 14 000 K for $\log g = 8$ causes significant changes in curves $F_{\rm He}(\lambda; \log\tau)$. The characteristic fluctuations of $F_{\rm He}(\lambda; \log\tau)$ in these figures are caused, exceptionally, by small fluctuations of the temperature and other atmospheric parameters in the corresponding table from Koester (1980), which was examined in detail in Mihajlov et al. (1995). However, the systematic increase of the temperature in the range $\log\tau \lesssim -2$ for about 1500 K causes a significant increase of the parameters $N(\rm He^+)/N(\rm He)$ and $N(\rm He_2^+)/N(\rm He^+)$, and, as a consequence, a significant increase of the absorption coefficients $\kappa_{\rm ia}^{(a)}$ and $\kappa_{\rm ia}^{(b)}$ of both absorption processes (3) and (4). This fact is reflected by the corresponding increase of the quantity $F_{\rm He}$ in Fig. 5 in the case of $T_{\rm eff} = 14\,000$ K with respect to Fig. 4 in the case of $T_{\rm eff} = 12\,000$ K.

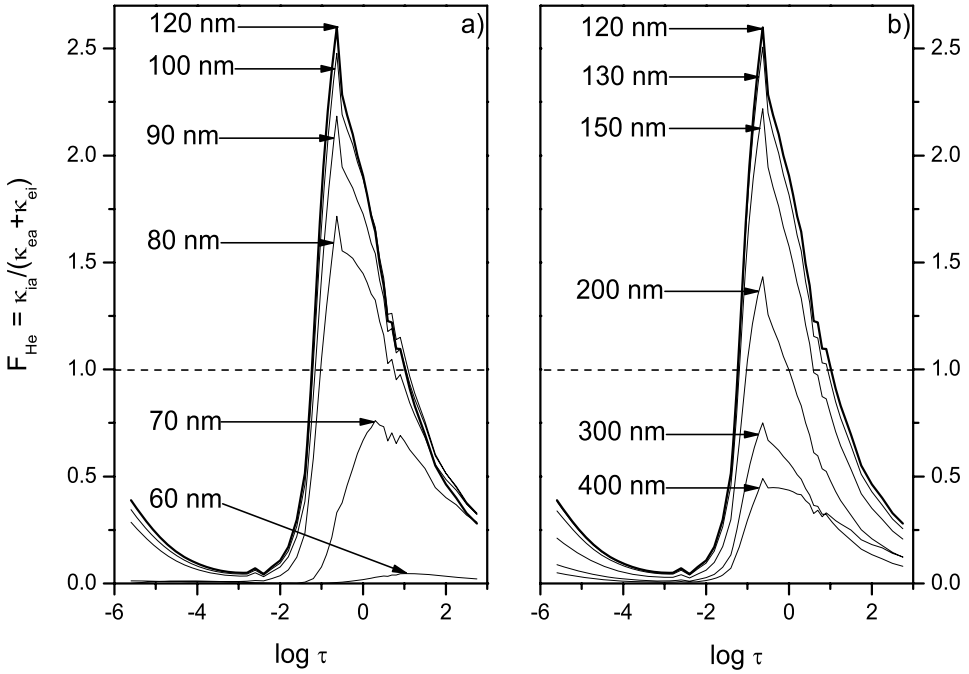

Figure 4. Behaviour of the quantity $F_{\rm He} = \kappa_{\rm ia}/(\kappa_{\rm ea} + \kappa_{\rm ei})$ within the atmosphere of a DB white dwarf in the case $\log g = 8$ and $T_{\rm eff} = 12\,000$ K.

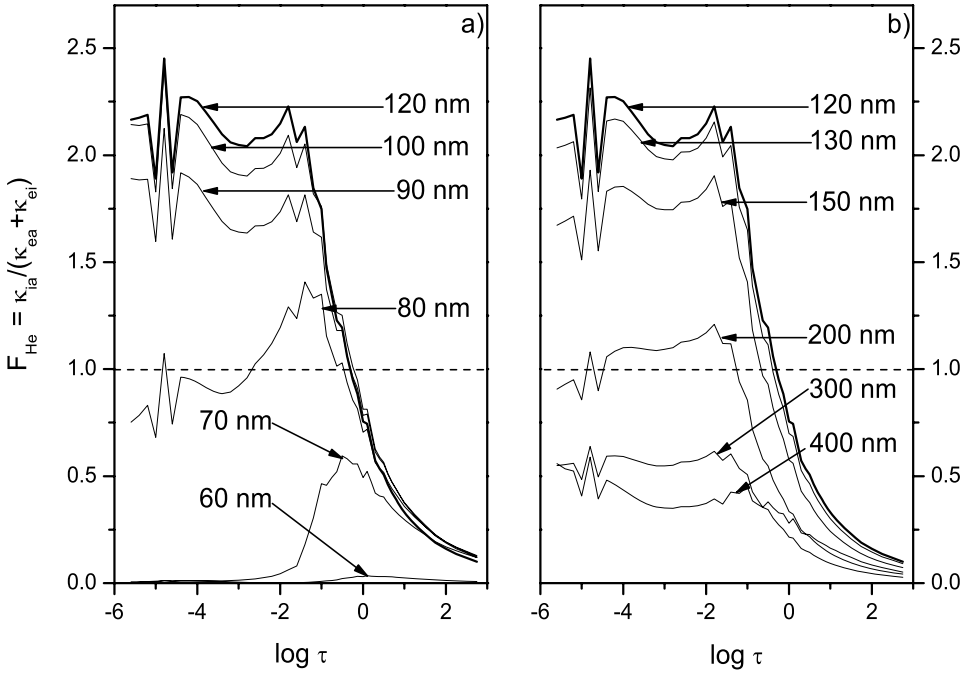

Figure 5. As Fig. 4, but for the case $\log g = 8$ and $T_{\rm eff} = 14000$ K.

Apart from that, the efficiency of the absorption processes (4) in the region $\lambda_{\rm He} < \lambda \leq \lambda_{\rm H}$ is compared with the efficiency of the hydrogen photoionization process (1), which is characterized by the spectral absorption coefficient $\kappa_{\rm H}(\lambda) \equiv \kappa_{\rm H}[\lambda; N({\rm H})]$ defined by

$$\kappa_{\rm H}(\lambda) = \sigma_{\rm phi}(\lambda) N({\rm H}), \tag{25}$$

where N(H) is the local density of atom H, and $\sigma_{\rm phi}(\lambda)$ the corresponding photoionization cross-section. Consequently, the relative efficiency of processes (4) and (7) for $\lambda \leq \lambda_{\rm H}$ can be characterized by the parameter $F_{\rm H}(\lambda)$, defined by

$$F_{\rm H}(\lambda) = \frac{\kappa_{\rm ia}(\lambda)}{\kappa_{\rm H}(\lambda)} = \frac{K_{\rm ia}(\lambda, T) N({\rm He}^+) N({\rm He})}{\sigma_{\rm phi}(\lambda) N({\rm H})}, \tag{26}$$

where the cross-section $\sigma_{\rm phi}(\lambda)$ is taken from Bethe & Salpeter (1957). It was found that the behaviour of $F_{\rm H}(\lambda)$ in all DB white dwarf atmospheres considered is qualitatively similar. Consequently, the behaviour of $F_{\rm H}(\lambda)$ is illustrated in Fig. 7 only for the

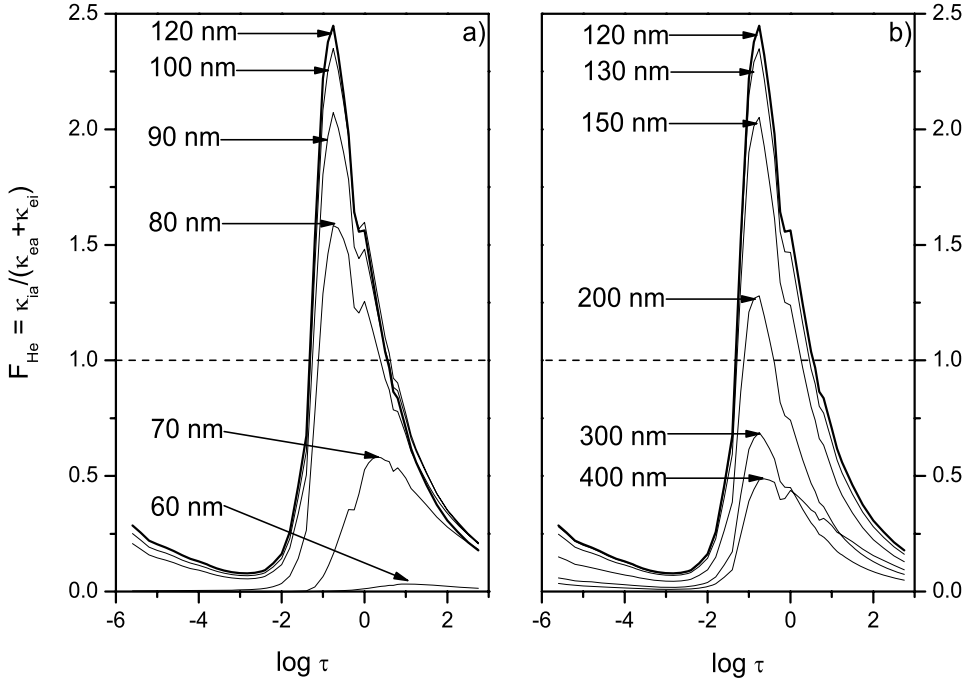

Figure 6. As Fig. 4, but for the case $\log g = 7$ and $T_{\rm eff} = 12\,000$ K.

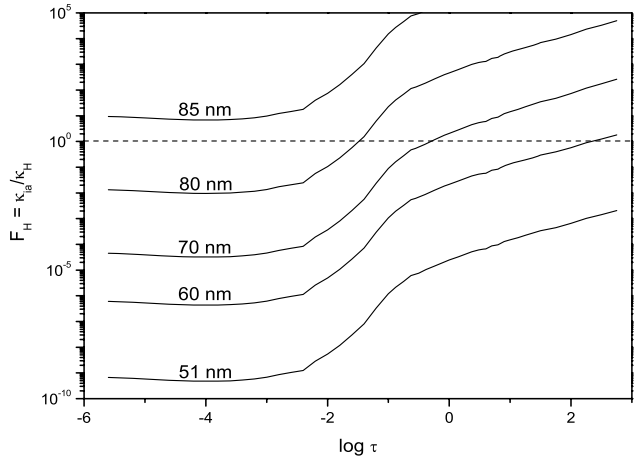

Figure 7. Behaviour of the quantity $F_{\rm H} = \kappa_{\rm ia}/\kappa_{\rm H}$ within the atmosphere of a DB white dwarf in the case $\log g = 8$ and $T_{\rm eff} = 12\,000$ K.

case $T_{\rm eff} = 12\,000$ K and $\log g = 8$. This figure shows that within the region $\lambda_{\rm He} < \lambda \lesssim 80$ nm the hydrogen photoionization process (7) should be treated as an important absorption process. Namely, for each λ from this region there is a significant part of the DB white dwarf atmosphere where process (7) dominates in comparison with the other absorption processes.

On the basis of Figs 4, 5, 6 and 7 one might expect that in the region $\lambda_{\rm He} < \lambda \leq 400$ nm the summary optical depth $\tau_{\rm sum}(\lambda; \log\tau)$ of the atmosphere layers considered, caused by all absorption processes relevant for continual spectra, should be significantly larger with respect to the optical depth caused by processes (1) and (2) only. For $\lambda_{\rm He} < \lambda \lesssim 70$ nm this increase should be caused by process (7), and for $\lambda \gtrsim 70$ nm by processes (4). Since only $\tau_{\rm sum}(\lambda; \log\tau)$ is necessary to describe the radiation transfer in the atmosphere considered, the behaviour of this quantity is examined here, supposing that only processes (4), (1), (2) and (7) cause the continuous absorption.

The contribution of processes (4) to the opacities of the DB white dwarf atmospheres considered is directly characterized by means of the quantity $\Delta\tau_{\rm ia}(\lambda; \log\tau)$, which represents the increase of the optical depth of the atmosphere layer considered that is caused by these processes themselves (see Mihajlov et al. 1995). We will characterize the contribution of the absorption processes considered to the opacity of DB white dwarf atmospheres by $\tau_{\rm sum}(\lambda; \log\tau)$ and the ratio $\Delta\tau_{\rm ia}(\lambda; \log\tau)/\tau_{\rm sum}(\lambda; \log\tau)$.

The behaviour of $\tau_{\rm sum}(\lambda; \log\tau)$ and $\Delta\tau_{\rm ia}(\lambda; \log\tau)/\tau_{\rm sum}(\lambda; \log\tau)$ is illustrated in Figs 8, 9 and 10 for the same cases: $T_{\rm eff} = 12\,000$ K and $\log\tau = 8$, $T_{\rm eff} = 12\,000$ K and $\log\tau = 7$, and $T_{\rm eff} = 14\,000$ K and $\log\tau = 8$. First of all, Figs 8(b)–10(b), which illustrate the behaviour of the ratio $\Delta\tau_{\rm ia}(\lambda; \log\tau)/\tau_{\rm sum}(\lambda; \log\tau)$, show that in the region $70\,{\rm nm} \lesssim \lambda \lesssim 400$ nm processes (4) give the dominant contribution to the opacity of the most important layer $-1 \lesssim \log\tau \lesssim 1$. This holds especially for the region $90\,{\rm nm} \lesssim \lambda \lesssim 150$ nm, where the contribution of processes (4) reaches ∼70 per cent. It means that this layer, according to Figs 8(a)–10(a), would be transparent in the absence of processes (4).

Also, Figs 8(a)–10(a) show that in the region $\lambda_{\rm He} < \lambda \lesssim 70$ nm the hydrogen photoionization process (7) causes the opacity of the layer $-1 \lesssim \log\tau \lesssim 1$. The influence of this process is especially strong in the case $\log g = 7$ and $T_{\rm eff} = 12000$ K, and weaker in the case $\log g = 8$ and $T_{\rm eff} = 14000$ K.

3 CONCLUSIONS

The results obtained allow the possibility of estimating which absorption processes give the main contribution to the opacity in DB white dwarf atmospheres in different spectral regions. Therefore, from our results it follows that the helium absorption processes (3)

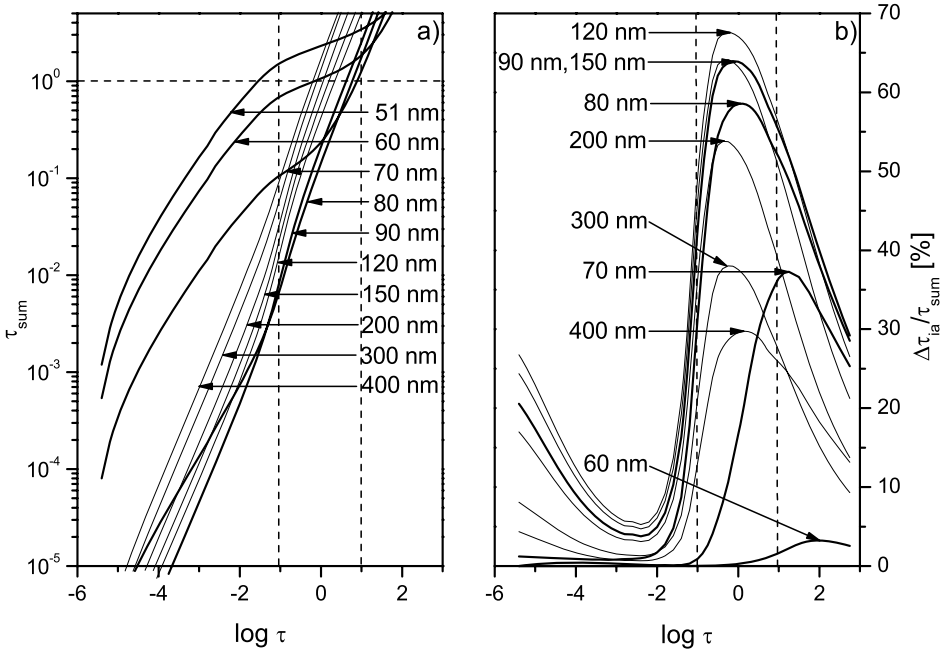

Figure 8. A DB white dwarf atmosphere in the case $\log g = 8$ and $T_{\rm eff} = 12000$ K: (a) the behaviour of the summary optical depth $\tau_{\rm sum}(\lambda; \log \tau)$ caused by the absorption processes (4), (1), (2) and (7); (b) the behaviour of the ratio $\Delta_{\rm ia}(\lambda; \log \tau)/\tau_{\rm sum}(\lambda; \log \tau)$ characterizing the relative contribution of processes (4) to the summary optical depth.

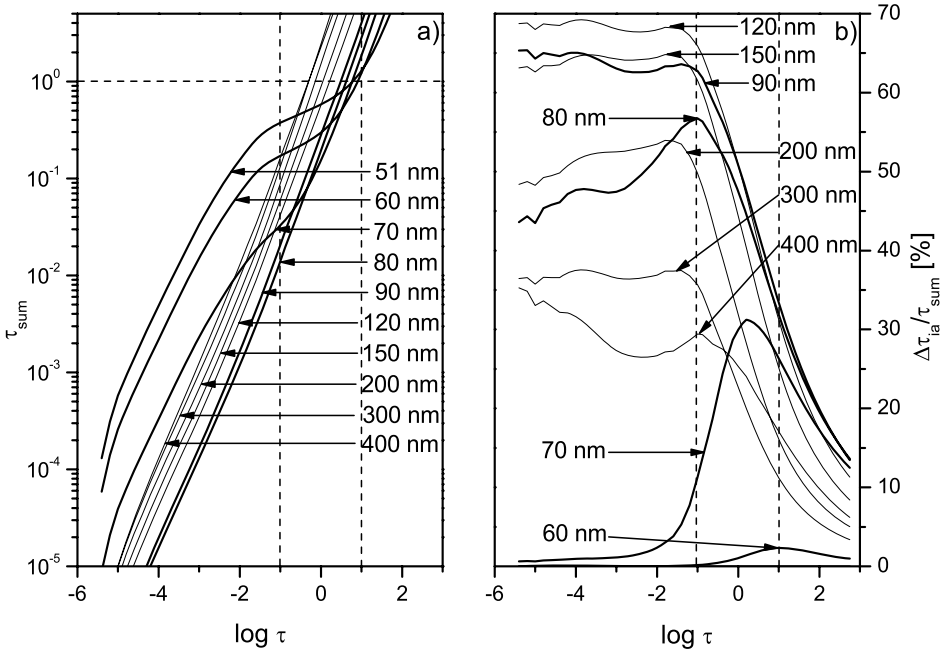

Figure 9. As Fig. 8, but for the case $\log g = 8$ and $T_{\rm eff} = 14\,000$ K.

and (4) are dominant in the region $70\,{\rm nm} \lesssim \lambda \lesssim 200\,{\rm nm}$, while in the region $\lambda > 200$ nm the He^- absorption processes (1) have the principal role, in contrast to the results presented in Stancil (1994). However, absorption processes (3) and (4) deserve to be included not only in the codes developed by e.g. Bergeron et al. (1995) but also in other DB white dwarf research.

Finally, it was shown that in the region $\lambda_{\rm He} < \lambda \lesssim 70\,{\rm nm}$, the hydrogen photoionization processes (7) take the dominant role in spite of the fact that the ratio of hydrogen and helium abundances in the DB white dwarf atmosphere considered is $1{:}10^5$. Consequently, the hydrogen photoionization processes (7) should also be included in DB white dwarf modelling. Moreover, this result opens the question of the eventual influence of metals, the abundance of which in the DB white dwarf considered is 1.5 times larger than that of hydrogen (Koester 1980).

We also note that the results obtained may be useful for the interpretation of observational data for DB white dwarfs. Namely, these results give the possibility of estimating from which atmospheric layers of DB white dwarfs the radiation at a given λ comes. This is important since the temperatures of these layers vary considerably with the Rosseland optical depth (τ), as follows from the models used (Koester 1980).

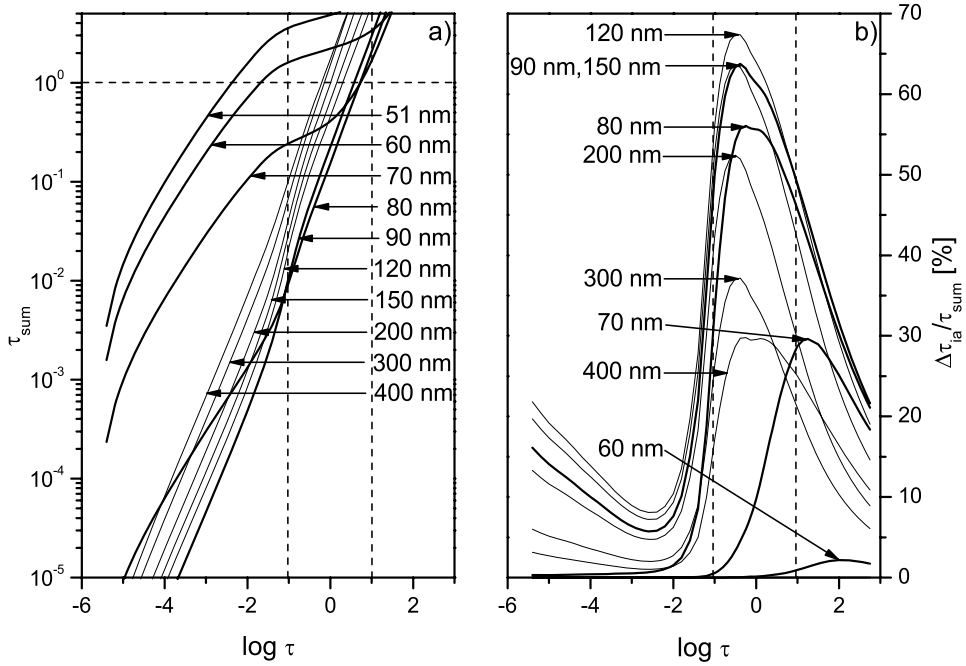

Figure 10. As Fig. 8, but for the case $\log g = 7$ and $T_{\rm eff} = 12\,000$ K.

ACKNOWLEDGMENTS

This work was supported by the Ministry of Science and Technological Development of Serbia as a part of the projects 'Radiation and transport properties of the non-ideal laboratory and ionospheric plasma' (Project number 141033) and 'Influence of collisional processes in astrophysical plasma line shapes' (Project number 146001).

REFERENCES

Bates D. R., 1952, MNRAS, 112, 40
Beauchamp A., Wesemael F., Bergeron P., Lebert J., Saffer R. A., 1996, in Jeffery C. S., Herber U., eds, ASP Conf. Ser. Vol. 96, Hydrogen-Deficient Stars. Astron. Soc. Pac., San Francisco, p. 295
Beauchamp A., Wesemael F., Bergeron P., 1997, ApJS, 108, 559
Bergeron P., Wesemael F., Beauchamp A., 1995, PASP, 107, 1047
Bethe H., Salpeter E., 1957, Quantum mechanics of one and two electron atoms. Springer Verlag, Berlin
Calamida A. et al. 2008, Mem. S. A. It., 79, 347
Dunning T. H., 1989, J. Chem. Phys., 90, 1007
John T. L., 1994, MNRAS, 269, 871
Kendall R. A., Dunning T. H., Harrison R. J., 1992, J. Chem. Phys., 96, 6769
Koester D., 1980, A&AS, 39, 401
Lebedev V. S., Presnyakov L. P., 2002, J. Phys. B: At. Mol. Opt. Phys., 35, 4347
Marsh T. R., Nelemans G., Steeghs D., 2004, MNRAS, 350, 113
Metropoulos A., Nicolaides A., 1991, Chem. Phys. Lett., 187, 487
Metropoulos A., Nicolaides A., Buenker R. J., 1987, Chem. Phys., 114, 1
Metropoulos A., Li Y., Hirsch G., Buenker R. J., 1992, Chem. Phys. Lett., 198, 266
Mihajlov A. A., Dimitrijević M. S., 1986, A&A, 155, 319
Mihajlov A. A., Dimitrijević M. S., 1992, A&A, 256, 305
Mihajlov A. A., Dimitrijević M. S., Ignjatović L. M., 1993, A&A, 276, 187
Mihajlov A., Dimitrijević M., Ignjatović L., 1994a, A&A, 287, 1026
Mihajlov A. A., Dimitrijević M. S., Ignjatović L. M., Djurić Z., 1994b, A&AS, 103, 57
Mihajlov A. A., Dimitrijević M. S., Ignjatović L. M., Djurić Z., 1995, ApJ, 454, 420
Mihajlov A. A., Ignjatović L. M., Sakan N. M., Dimitrijević M. S., 2007, A&A, 437
Mihalas D., 1978, Stellar Atmospheres. W.H. Freeman, San Francisco
Patch R. W., 1969, J. Quant. Spectrosc. Radiative Transfer, 9, 63
Sobel'man I. I., 1979, Atomic Spectra and Radiative Transitions. Springer Verlag, Berlin
Somerville W. B., 1965, ApJ, 141, 811
Stancil P. C., 1994, ApJ, 430, 360
Stancil P. C., Bab J. F., Dalgarno A., 1993, ApJ, 414, 672
Werner H.-J. et al., 2006, MOLPRO, version 2006. 1, a package of ab initio programs, see http://www.molpro.net

This paper has been typeset from a TEX/LATEX file prepared by the author.